

THE EFFECT OF TEMPERATURE ON THE DEFORMATION STRUCTURE OF SINGLE CRYSTAL NICKEL BASE SUPERALLOYS

M.Dollar[‡] and I.M.Bernstein[‡]

Carnegie Mellon University, Pittsburgh, PA 15213

[‡] now at the Illinois Institute of Technology, Chicago, IL 60616

ABSTRACT

The temperature dependence of the yield and flow stress was analyzed in the superalloys PWA 1480 and CMSX-2. From measured dislocation densities at different strains and temperatures, flow stresses were accurately predicted from an extended Copley and Kear model (5). Differences in the strain response of the two alloys were described.

I. INTRODUCTION

Nickel-base superalloys offer desirable creep strength, thermal fatigue stress, oxidation resistance, and hot corrosion resistance [1,2], making them important materials for gas turbine engine applications. Recently, single-crystal nickel-base superalloys have been developed, in order to remove grain boundary strengthening elements, providing an increase in the incipient melting temperature [3,4]. This permits solution heat treatments to be carried out at higher temperatures which both improves materials homogeneity and dissolves coarse primary particles.

The ability to use these superalloys at progressively higher temperatures has encouraged a number of recent studies designed to fully characterize their high temperature properties [3,4]. What is lacking are a sufficient number of attempts to understand the fundamentals of the deformation processes in superalloys, particularly the effects of temperature on superalloy deformation and properties. Earlier efforts were at the best incomplete [5,6]. This perceived gap has led to the present research. Its aim has been to clarify the role of temperature on the development of deformation structure and tensile properties in PWA 1480 and CMSX-2, produced by Pratt and Whitney Aircraft and Cannon-Muskegon Corporation, respectively, both being considered for use in the space shuttle main engine [7].

II. EXPERIMENTAL PROCEDURES

The chemical compositions of the superalloys investigated in the present study are given in Table I. They were provided in the form of bars, both with longitudinal orientations within 10° of [001]. Tensile samples were then machined in accordance with ASTM specification,

Superalloys 1988
Edited by S. Reichman, D.N. Duhl,
G. Maurer, S. Antolovich and C. Lund
The Metallurgical Society, 1988

selecting only bars with orientations $5^\circ \pm 1^\circ$ from [001], to minimize any influence of variations in orientation. The materials were heat treated according to schedules reported in Table II.

Table I. Alloy Compositions (wt. pct.)

	Al	Co	Cr	Ta	Ti	W	Mo	Ni
PWA 1480	4.8	5.3	10.4	11.9	1.3	4.1	---	bal.
CMSX-2	5.6	4.6	8.0	6.0	1.1	8.0	0.6	bal.

Tensile testing was conducted on an Instron machine at temperatures from 20°C to 800°C at an initial strain rate of $1.2 \times 10^{-3} \text{ s}^{-1}$. Interrupted tensile tests to selected strain levels were also carried out to study the development of deformation structure.

TABLE II. The heat treatment procedures for PWA 1480 and CMSX-2 superalloys

<u>PWA 1480</u>	<u>CMSX-2</u>
1285°C / 4h	1315°C / 3h
1080°C / 4h	1050°C / 16h
870°C / 32h	850°C / 48h

Discs for transmission electron microscopy (TEM) were prepared from undeformed heat treated materials, as well as from tensile samples strained to different strain levels at different temperatures. The discs were cut perpendicular to the tensile axis, as well as parallel to {111} planes. Thin foils were prepared by twin-jet electropolishing and examined at 120kV, in a Phillips 420 microscope.

III. EXPERIMENTAL RESULTS

A. Microstructure

The general characteristics of the macrostructure and microstructure produced by the heat treatments reported in Table II in both alloys have previously been presented (CMSX-2 [8], PWA 1480 [6]).

In both, a high volume fraction of 65% cuboidal, ordered particles in a matrix were observed, with an edge length of $500 \pm 100 \text{ nm}$ ($400 \pm 150 \text{ nm}$ in PWA 1480). TEM failed to reveal the presence of γ/γ' interfacial dislocations, in accordance with the reported small γ/γ' misfit at room temperature of 0.14% for CMSX-2 [9] and 0.28% for PWA 1480 [6].

B. Mechanical Properties

The true values of the yield stress, flow stress and ultimate tensile stress at 1% strain, versus temperature for PWA 1480 are shown in Fig.1. The yield stress at room temperature of about 1000 MPa decreases quite significantly with increasing temperature until 400°C, above which the yield stress then increases, peaking at 730°C. Beyond 730°C, the strength again drops. The other stresses behave similarly, (Fig.1), compatible with the strong work hardening of the alloy over all strains and temperatures examined.

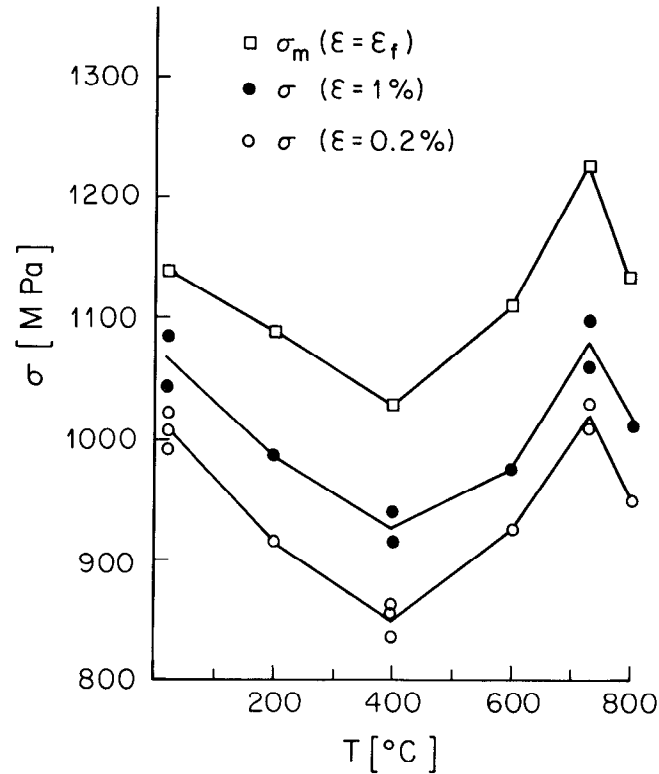


Figure 1. The effect of temperature on the yield stress, the flow stress for the strain of 0.01 and the ultimate tensile stress in PWA 1480.

The yield stress at room temperature for CMSX-2 is slightly smaller than PWA 1480 and in addition there is no drop in strength beyond this temperature. In fact, the yield stress is the same at 20 and 400°C, with a peak yield stress peak at 730°C (as in PWA 1480). In contrast with PWA 1480, much less work hardening is observed in CMSX-2.

C. Deformation structures

The development of dislocation structure at different stress levels was investigated in PWA 1480 at 20, 400 and 730°C in [001] oriented foils, unless indicated otherwise. This is the most appropriate orientation to observe simultaneously the deformation behavior of both phases in [001] single crystals which contain particles with their faces parallel to the [001] growth direction.

At room temperature and a strain of 0.24%, significant dislocation activity was already present in the matrix (Fig.2), in contrast with the γ' phase, where dislocations were observed only occasionally. The matrix dislocations were determined to have a Burgers vector of $\langle 110 \rangle$ and usually were present as loosely coupled pairs, suggesting that they are superdislocations trapped in the matrix at the earliest stages of plastic deformation.

With increasing strain the dislocation density increases in both the matrix and the precipitates, but is still substantially higher in the matrix, as illustrated in Fig. 3, for a strain of 1.2%. Dislocation densities were measured in the matrix for strains of 0.24, 1.2, and 3.5% (the strain to failure), and are given in Table III.

The dislocation structure in a foil cut parallel to $\{111\}$ planes after 1.2% strain is shown in Fig.4. The use of this orientation permits superdislocations to be shown on their slip planes and are seen to be straight $\langle 110 \rangle$ superdislocations of screw character (i.e. parallel to $\langle 110 \rangle$ directions). By the use of weak-beam dark field imaging the mean separation of superpartials was found to be 4.8 ± 0.8 nm.

TABLE III. The results of dislocation density measurements in PWA 1480 superalloy

Deformation temperature (°C)	Strain (%)	Location	Dislocation density (cm ²)	Standard deviation (cm ²)
20	0.24	γ	1.3×10^{10}	0.7×10^{10}
20	1.2	γ	5.2×10^{10}	2.0×10^{10}
20	3.5	γ	1.4×10^{11}	3.6×10^{10}
400	1.8	γ	4.2×10^{10}	1.7×10^{10}
400	1.8	γ'	5.7×10^{10}	2.8×10^{10}

In contrast with room temperature, at 400°C no significant superdislocation trapping in the matrix was found, as can be seen by comparing Fig. 5, representing the typical dislocation structure at 400°C for a strain of 1.8% with Fig. 3. The corresponding dislocation densities measured in both the matrix and in the γ' phase are given in Table III.

In contrast with both 20 and 400°C, at 730°C, the superdislocations while still exhibiting predominantly screw character, are no longer straight, as shown in Fig. 6, representing a typical dislocation structure for $\epsilon = 2.0\%$.

The development of the dislocation structure in CSMX-2 was investigated at room temperature only. At the earliest stages of plastic deformation, numerous dislocations were found in the matrix, with occasional superdislocation pairs observed in the precipitates. Detailed analysis indicates that, as in PWA 1480, the matrix dislocations are most likely superdislocations trapped in the disordered phase.

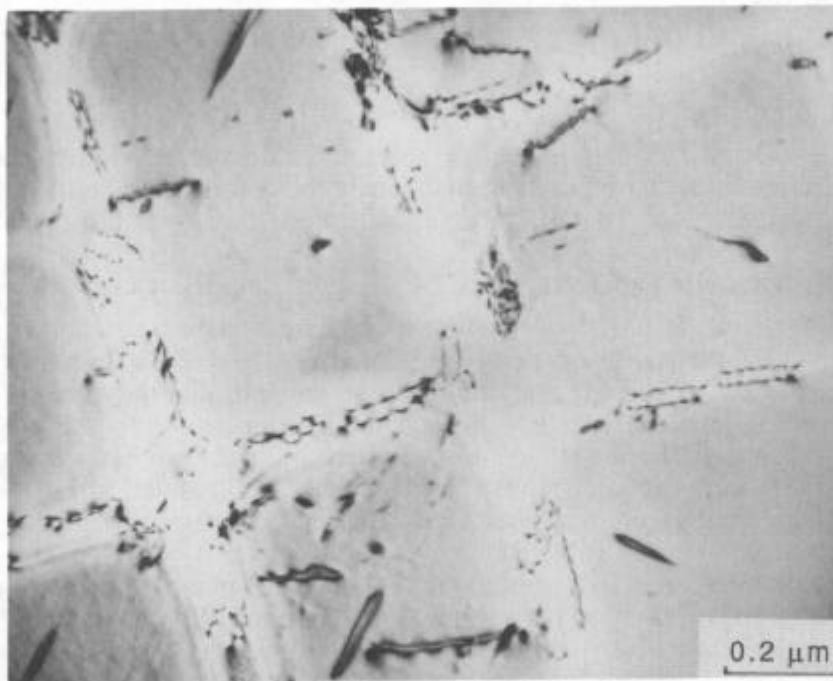


Figure 2. TEM micrograph, PWA 1480, $T_{\text{def}} = 20^\circ\text{C}$, $\epsilon_P = 0.24\%$, the foil normal is [001].

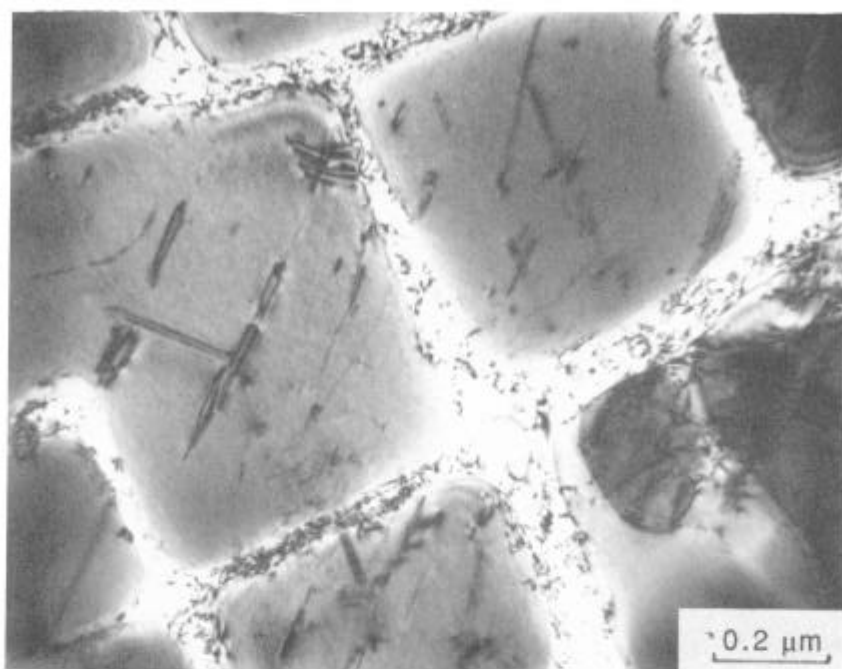


Figure 3. TEM micrograph, PWA 1480, $T_{\text{def}} = 20^{\circ}\text{C}$, $\epsilon_p = 1.2\%$, [001] foil.



Figure 4. TEM micrograph, PWA 1480, $T_{\text{def}} = 20^{\circ}\text{C}$, $\epsilon_p = 1.2\%$, [111] foil.

At higher strains the comparative dislocation structure in both alloys is remarkably different. In CMSX-2 the dislocation distribution is more uniformly distributed through both the γ and γ' . There appear to be no barriers to prevent the superdislocations from moving over appreciable distances, suggesting the mean free path of superdislocations is significantly greater in CMSX-2 than in PWA 1480.

The mean separation of superpartials was also measured for CMSX-2 and found to be 4.6 ± 0.3 nm in CMSX-2, not significantly different from PWA 1480.

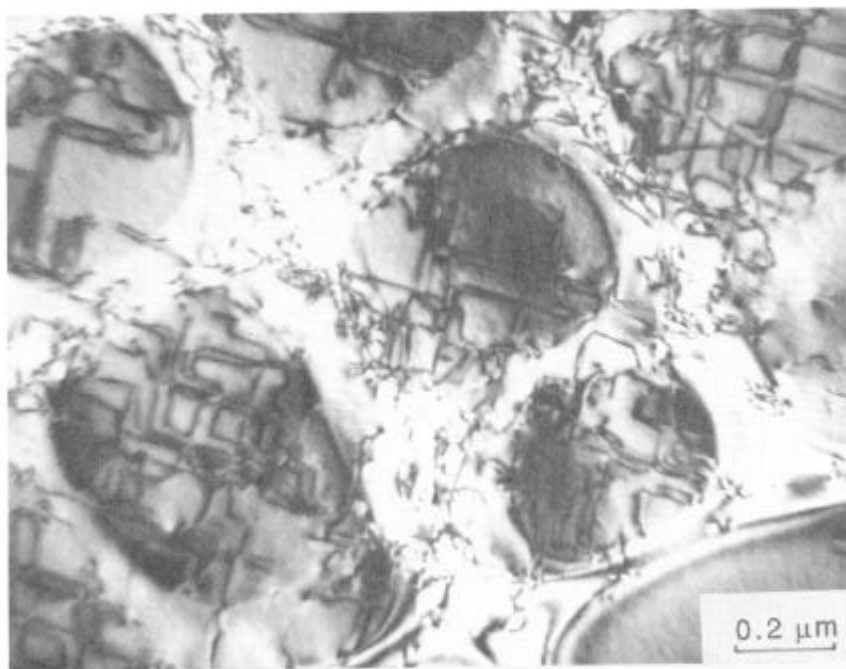


Figure 5. TEM micrograph, PWA 1480, $T_{\text{def}}=400^{\circ}\text{C}$, $\epsilon_p=1.8\%$, [001] foil.

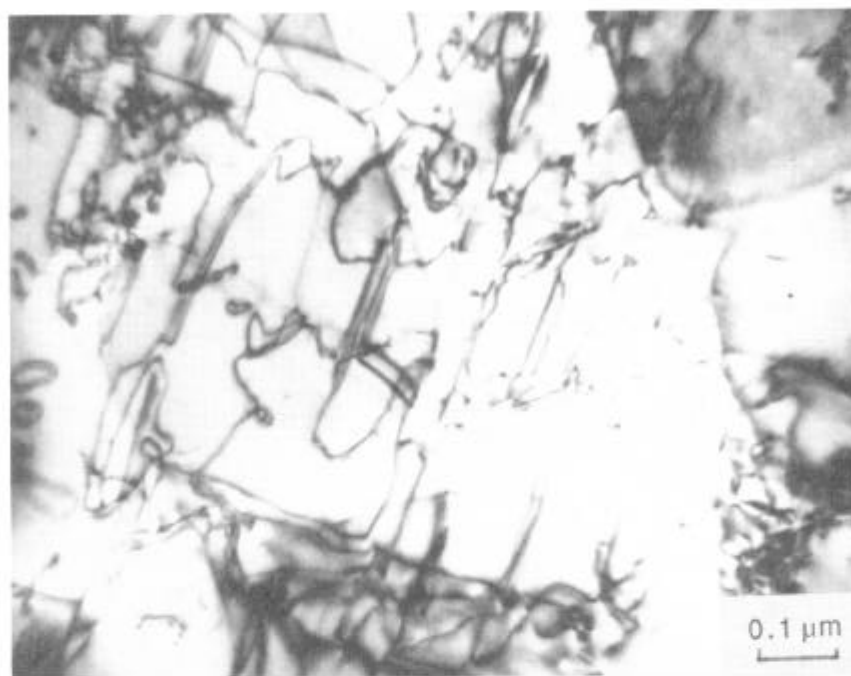


Figure 6. TEM micrograph, PWA 1480, $T_{\text{def}}=730^{\circ}\text{C}$, $\epsilon_p=2.0\%$, [001] foil.

IV. DISCUSSION

A reasonable approach for a discrete two phase single crystal superalloy is to try to calculate its yield stress from the yield stresses of its constituent single phases. For example with PWA 1480 appropriate data is available [5,10]. The yield stress, σ_p , versus temperature of a single-phase alloy of chemical composition similar to that of γ in PWA 1480, is shown in Fig.7 (curve c), as is the yield stress, σ_M , as a function of temperature (curve a) of a commercial,

solution hardened Hasteloy X alloy, of chemical composition similar to that of the γ phase in PWA 1480 (for both, the critical resolved shear stresses (CRSS) for $\{111\}\langle 110 \rangle$ primary octahedral slip are multiplied by the reciprocal of the Schmid factor $M = 0.41$, the value appropriate for the $\langle 001 \rangle$ orientation [5,11]). The experimental values of the yield stress for PWA 1480 are shown in Fig. 7 as well. It is apparent that the use of any conventional model for yielding in two-phase alloys [12] can not allow a quantitative prediction of the yield behavior of the superalloy, since the resultant stress, as calculated by conventional models, would never exceed that of the harder phase. Any successful explanation has to account for the strong strengthening of the superalloy in comparison to its ordered phase.

Models have been developed by Huther and Reppich [13] and by Copley and Kear [5], specifically for alloys strengthened by large, coherent, ordered particles. The latter authors considered both the leading and trailing dislocations (forming a superdislocation) in the balance of forces, and the additional strengthening of a superalloy arises from the energy that must be supplied as a superdislocation passes from the disordered matrix into the ordered particle. The CRSS, σ_C , is given by:

$$\tau_C = \left(\frac{E_A}{2b} \right) - \left(\frac{T}{br} \right) + [0.41(\tau_M + \tau_P)] \quad (1)$$

where: E_A = antiphase boundary energy, b = dislocation Burgers vector, T = dislocation line tension, r = particle radius, τ_M = CRSS of γ and τ_P = CRSS of γ' .

We can apply Eq. (1) to calculate first the yield stress of PWA 1480 at room temperature, and then to model the temperature dependence of the yield stress following Copley and Kear's procedure for the MAR M200 superalloy [5].

At room temperature: $G = 57$ GPa (G is estimated as G_{Ni} parallel to $\{111\}\langle 110 \rangle$ [14]), $b = 2.5 \times 10^{-8}$ cm, and $r = 0.15 \times 10^{-4}$ (as measured from TEM results). T was calculated from $T = Gb^2/2$ [15], E_A was calculated from the relationship developed in reference [16]:

$$E_A = \frac{c G b^2}{2 \pi d} \quad (2)$$

where: c = constant equal to unity for screw dislocations [16], and d = the mean distance between superpartials, measured to be 4.8 nm. A value of $E_A = 118$ mJ/m² was estimated. Using $\tau_M = 180$ MPa and $\tau_P = 115$ MPa from [5], the CRSS of PWA 1480 predicted by Eq.(1) then equals 317 MPa. Thus, the predicted yield stress:

$$\sigma_C = M^{-1} \tau_C \quad (3)$$

equals 773 MPa for Schmid factor $M=0.41$ compared to the experimental value of 1013 MPa.

To model the temperature dependence of the yield stress for [001] oriented PWA 1480 crystals, the τ_M and τ_P versus T relationships were used exclusively by assuming that the other parameters appearing in Eq. (1) were temperature-independent. The resultant yield stress-temperature relationship obtained ($M = 0.41$) is shown in Fig. 7 as $\tau_C = \tau_1 + \tau_2$ (curve d).

The above approach successfully predicts to within almost 10% why at temperatures above 400°C superalloys in general, and PWA 1480 in particular, are strengthened in excess of the intermetallic compounds forming their precipitates. However, the approach does not explain why the experimental yield stress at room temperature is much higher than predicted, and also why there is a significant drop of the yield stress with increasing temperature till 400°C.

To better model this region of the yield stress-temperature regime, we have made use of our TEM studies, which showed the existence of a substantial dislocation density in the matrix slightly above yield at room temperature. In as much as Eq. (3) was derived under the implicit

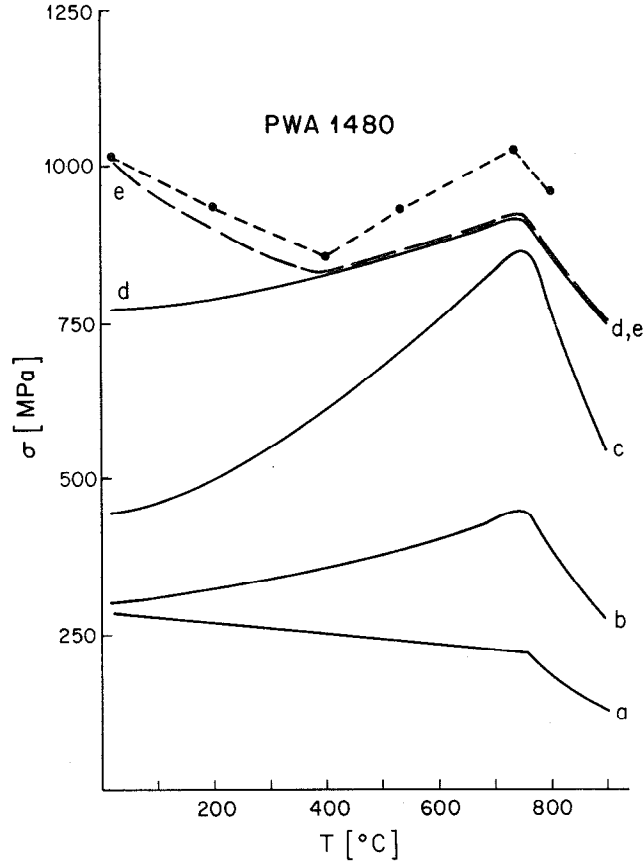


Figure 7. The plot of yield stress versus temperature curves (a) τ_M - yield stress of γ (b) τ_P - yield stress of γ' (c) $\tau_1 = .41(\tau_M + \tau_P)$ (d) τ_C (Eq. 3) (e) σ_Y of PWA 1480. Experimental data represented by dots.

assumption that a moving superdislocation, passing from the matrix into the γ' phase does not interact with other dislocations, it can not reflect the dislocation accumulation in the matrix which inevitably strengthens the superalloy. From conventional work hardening theories [17,18], the additional strengthening can be given as:

$$\delta\sigma = M^{-1} \alpha G b \rho^{1/2} \quad (4)$$

where: α = constant, typically about 0.5 and ρ = total dislocation density.

The yield stress, σ_Y , can be now postulated to consist of two components: σ_C (Eq. (3)) and $\delta\sigma$ (Eq. (4)), thus:

$$\sigma_Y = M^{-1} \left\{ \left(\frac{E_A}{2b} \right) - \left(\frac{T}{br} \right) + [0.41(\tau_M + \tau_P)] + \alpha G b \rho^{1/2} \right\} \quad (5)$$

Taking $\rho = 1.3 \times 10^{-10} \text{ cm}^{-2}$ at yield (Table III) and fitting the value of $\alpha = 0.6$, we now estimate the yield stress at room temperature to be 1010 MPa, in excellent agreement with the experimental yield stress. Clearly this exactness results from the choice of $\alpha = 0.6$, a very reasonable value in agreement with many work hardening theories. Since above 400°C no pronounced dislocation accumulation was observed in the matrix, the incremental strengthening

given by Eq. (4) is negligible and we assume that it decreases from 98 MPa at 20°C to zero at 400°C. Using this approach, curve e in Fig. 7 is obtained, and is in excellent agreement with experiment.

To test the generality of the approach used for PWA 1480 the yield stress versus temperature relationship for CMSX-2 was also calculated. The experimental data is re-shown in Fig. 8 and the yield stress is calculated from Eqs.(1-3), using measured $r = 0.18 \times 10^{-4}$ cm and $d = 4.6$ nm, calculating $E_A = 123$ mJ/m², and taking the same $\tau_M(T)$ and $\tau_P(T)$ relationships, G and b as for PWA 1480. The predicted σ_C versus T relationship for [001] oriented crystals ($M=0.41$) is shown in Fig. 8 and agrees with experiment to within 11% over the entire temperature range, in contrast to PWA 1480.

It is clear, and supported by TEM results, that in CMSX-2, unlike PWA 1480, strength increases due to work hardening do not occur. While at small strains some superdislocations are trapped in the matrix of CMSX-2, the tendency is much less pronounced than for PWA 1480. For instance, at room temperature the dislocation density in the matrix of CMSX-2 at 0.8% strain is significantly lower than that in the matrix of PWA 1480 at 0.24% strain.

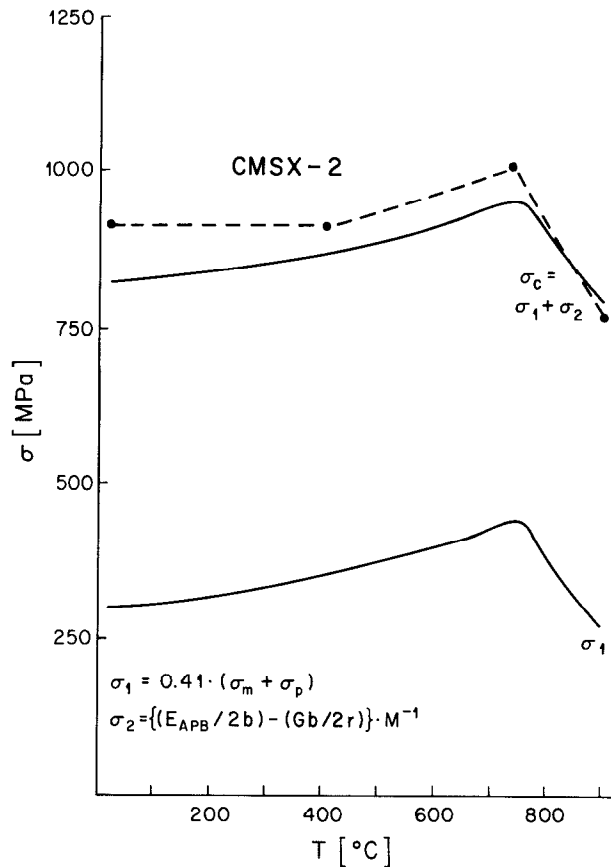


Figure 8. Plot of σ_Y versus temperature. The σ_C curve is predicted for CMSX-2. Experimental data represented by dots.

V. CONCLUSIONS

1. PWA 1480 and CMSX-2 superalloys are strengthened in excess of their constituent phases. This is a consequence of the fact that energy must be supplied as a superdislocation passes from the disordered matrix into the ordered particle. If this results in the trapping of superdislocations in the matrix, an additional increment of strengthening ensues.
2. The yield stress versus temperature relationships in both superalloys can be reasonably reproduced from existing or extended phenomenological models, taking account of both theoretical considerations and structural observations.
3. The development of dislocation structure is different in the two superalloys (as is their ductility and work hardening). The reasons for such behavior is yet to be established.

REFERENCES

1. R.F.Decker and T.S.Sims, in: *The Superalloys*, T.S.Sims and W.C.Hagel (eds.), John Wiley and Sons, New York 1972, p.33
2. T.S.Sims, in: *Superalloys '84*, Proc.5th International Symposium on Superalloys, M.Gell et al. (eds.), The Metallurgical Society Publication, New York 1984, p.399
3. M.Gell, D.N.Duhl, A.F.Giamei, in: *Superalloys '80*, Proc.4th International Symposium on Superalloys, J.K.Tien et al. (eds.), American Society for Metals, Metals Park Ohio 1980, p.205
4. M.Gell, D.N.Duhl, D.K.Gupta and K.D.Sheffer, *J. of Metals*, **39**, 11 (1987)
5. S.M.Copley and B.H.Kear, *Trans. of AIME*, **239**, 984 (1967)
6. W.W.Milligan and S.D.Antolovich, *Metall.Trans.*, **18A**, 85 (1987)
7. W.T.Chandler, Final Report - Materials for Advanced Rocket Engine Turbopump Turbine Blades, Rockwell International Rocketdyne Division, Canoga Park, CA, 1984
8. C.L.Baker, J.Chene, I.M.Bernstein and J.C.Williams, *Metall.Trans.*, **19A**, 73, (1988)
9. P.Caron and T.Khan, *Mat. Sci.Eng.*, **61**, 173 (1983)
10. B.J.Piercay and R.W.Smashey, *PWA Report 65-018*, Pratt and Whitney Aircraft, North Haven Conn. 1965
11. D.M.Shah and D.N.Duhl, in: *Superalloys '84*, Proc.5th International Symposium on Superalloys, M.Gell et al. (eds.), The Metallurgical Society Publication, New York 1984, p.105
12. R.W.K.Honeycombe, *The Plastic Deformation of Metals*, Edward Arnoldt Publ., London 1984, p.252
13. W.Huether, B.Reppich, *Z.Metallkunde*, **69**, 628 (1978)
14. J.F.Nye, *Physical Properties of Crystals*, Oxford University Press, London 1957, p.148
15. D.Hull and D.J.Bacon, *Introduction to Dislocations*, Pergamon Press, Oxford 1984
16. J.T.M. De Hosson, *Mat.Sci. Eng.*, **81**, 515 (1986)
17. D.Kuhlmann-Wilsdorf, in: *Work Hardening in Tension and Fatigue*, A.W.Thompson (ed.), The Metallurgical Society Publication, New York 1976, p.1
18. D.Kuhlmann-Wilsdorf, *Metall.Trans.*, **16A**, 2091 (1985)

VI. ACKNOWLEDGEMENTS

The authors are grateful to Mr. W.S.Walston for his technical assistance and many fruitful discussions. This research was supported by NASA-Lewis Research Center under the technical direction of Dr. R. Dreshfield.